

Lymph Node Colonization Dynamics after Oral *Salmonella* Typhimurium Infection in Mice

Patrick Kaiser¹, Emma Slack¹, Andrew J. Grant², Wolf-Dietrich Hardt^{1*}, Roland R. Regoes^{3*}

1 Institute of Microbiology, ETH Zurich, Zurich, Switzerland, **2** Department of Veterinary Medicine, University of Cambridge, Cambridge, United Kingdom, **3** Institute of Integrative Biology, ETH Zurich, Zurich, Switzerland

Abstract

An understanding of how pathogens colonize their hosts is crucial for the rational design of vaccines or therapy. While the molecular factors facilitating the invasion and systemic infection by pathogens are a central focus of research in microbiology, the population biological aspects of colonization are still poorly understood. Here, we investigated the early colonization dynamics of *Salmonella* enterica subspecies 1 serovar Typhimurium (*S. Tm*) in the streptomycin mouse model for diarrhea. We focused on the first step on the way to systemic infection — the colonization of the cecal lymph node (cLN) from the gut — and studied roles of inflammation, dendritic cells and innate immune effectors in the colonization process. To this end, we inoculated mice with mixtures of seven wild type isogenic tagged strains (WITS) of *S. Tm*. The experimental data were analyzed with a newly developed mathematical model describing the stochastic immigration, replication and clearance of bacteria in the cLN. We estimated that in the beginning of infection only 300 bacterial cells arrive in the cLN per day. We further found that inflammation decreases the net replication rate in the cLN by 23%. In *ccr7*^{-/-} mice, in which dendritic cell movement is impaired, the bacterial migration rate was reduced 10-fold. In contrast, *cybb*^{-/-} mice that cannot generate toxic reactive oxygen species displayed a 4-fold higher migration rate from gut to cLN than wild type mice. Thus, combining infections with mixed inocula of barcoded strains and mathematical analysis represents a powerful method for disentangling immigration into the cLN from replication in this compartment. The estimated parameters provide an important baseline to assess and predict the efficacy of interventions.

Citation: Kaiser P, Slack E, Grant AJ, Hardt W-D, Regoes RR (2013) Lymph Node Colonization Dynamics after Oral *Salmonella* Typhimurium Infection in Mice. PLoS Pathog 9(9): e1003532. doi:10.1371/journal.ppat.1003532

Editor: Bruce R. Levin, Emory University, United States of America

Received: January 25, 2013; **Accepted:** June 17, 2013; **Published:** September 19, 2013

Copyright: © 2013 Kaiser et al. This is an open-access article distributed under the terms of the Creative Commons Attribution License, which permits unrestricted use, distribution, and reproduction in any medium, provided the original author and source are credited.

Funding: RRR gratefully acknowledges funding from the Swiss National Science Foundation (grant number 315230-130855), the experimental work was supported by the Swiss National Science Foundation (grant 310030-132997/1 to WDH), and ES is supported by an SNF ambizione fellowship. The funders had no role in study design, data collection and analysis, decision to publish, or preparation of the manuscript.

Competing Interests: The authors have declared that no competing interests exist.

* E-mail: wolf-dietrich.hardt@micro.biol.ethz.ch (WDH); roland.regoes@env.ethz.ch (RRR)

Introduction

Understanding the population biological aspects of how a pathogen colonizes its host is crucial for prevention of infection. Only if we know where a pathogen enters, which anatomical compartments it colonizes, where and how fast it replicates, migrates, and gets killed, will we be able to optimally design interventions that block this process. Just as there are molecular Achilles' heels of pathogens, population dynamical parameters exist that characterize vulnerabilities of the infection process. Combining the knowledge of molecular mechanisms with an understanding of the population dynamics of an infection thus holds great promise for the design of vaccines and therapy. For most pathogens, however, the population biological aspects of infection are not well understood.

The population dynamics of pathogens within the host has been investigated most extensively for viruses, in particular for Human and Simian Immunodeficiency Viruses. We know how this virus enters [1], diversifies [2,3], and is controlled by the immune response early in infection [4–8]. Less is known about the anatomical aspects of early colonization of humans because this requires frequent sampling of various compartments. In animal models, population dynamic parameters characterizing the anatomical spread of the virus are starting to be determined [9].

Similar insights have been obtained for influenza virus [10] and Hepatitis C Virus [11].

The study of the colonization dynamics of bacterial pathogens has an impressive early history. Meynell & Stocker used pairs or triplets of differentially marked strains of *Salmonella* to investigate if bacterial cells initiate an infection independently of each other [12,13]. Later Moxon & Murphy extended this approach to *Haemophilus influenzae* [14]. By sampling bacteria from different compartments, they obtained qualitative information on the colonization pathways of the pathogen.

Today we have much better tools to monitor bacterial spread and replication at our disposal, and advanced population dynamical methods are being used to understand how infections unfold within their hosts [15]. However, these tools and methods have not been extensively used to analyze bacterial colonization dynamics. This is surprising because of the long history of this question, and the importance for these processes for vaccination and treatment.

Nevertheless, there are a few notable studies on the colonization of host by bacterial pathogens. Recently, Margolis & Levin [16] presented an extended study of the system used by Moxon & Murphy. In particular, they investigated if colonization relied on bacterial evolution. Furthermore, the colonization pathways of *Yersinia pseudotuberculosis* has been investigated qualitatively [17].

Author Summary

Like humans, pathogens have a demography. Within their hosts, they migrate, replicate, and die. Understanding these processes quantitatively can help designing vaccines and treatment by identifying vulnerabilities of the pathogen population. For most pathogens, however, quantitative information on how they replicate and spread in their hosts is lacking. Here, we investigate the early colonization of hosts by *Salmonella* bacteria after oral infection in a mouse model for complicated *Salmonella* diarrhea. To estimate migration and replication rates, we infected the mice with mixtures of identical, but distinguishable strains of the bacterium and analyzed the results with a mathematical model that describes the demography of the bacterial population. Random loss of some of these strains during colonization of the mice allows us to estimate migration rates between anatomical compartments. We find that approximately 300 bacteria migrate per day from the gut to the cecal lymph node – the first step towards systemic infection. We further investigate how bacterial migration and replication is affected by inflammation and various agents of the immune system. Our study provides unprecedented information on the colonization dynamics of this bacterial infection and introduces a framework for further improving therapy and vaccination.

The arguments in this study are reminiscent of Moxon & Murphy's early study on the colonization dynamics of *H. influenzae*. Lastly, Grant et al. presented a quantitative study on the dynamics of *Salmonella* infection following intravenous inoculation of mice [18].

In the present study, we define the early population dynamics in a mouse model for *Salmonella* diarrhea [19,20]. After inoculation of the mice, the bacterial population grows to a population size of about one billion cells in the gut. From the gut, bacteria colonize the cecal lymph node (cLN), and subsequently spread throughout the body of the mice from there. As the migration from the gut to the cLN initiates systemic infection, we focus on this step in the present study.

We were primarily interested in the rate at which the bacteria migrate from the gut to the cLN, and in the growth rate of the bacterial population in that compartment. To estimate these key population biological parameters we used inocula containing multiple wild type isogenic tagged strains (WITS) that have been used to elucidate population biological characteristics of bacterial pathogens in other systems [17,18]. The mixed inocula revealed the stochasticity in the colonization process, which we could exploit for parameter estimation. To determine the population biological significance of inflammation and dendritic cells, we conducted experiments with mutant strains of *S. Tm* with well characterized virulence defects and different mice strains with known deficiencies in pathogen handling.

Results

Rationale and approach

Determining the migration, replication and clearance rates of bacteria *in vivo* constitutes a challenge. While the bacterial population size can be measured in many anatomical compartments, this measure is a complex composite of migration, replication and clearance, and hence does not allow quantifying the rates at which these processes occur. Therefore, we have developed a novel approach combining experimental infection

with mixed inocula and mathematical modeling to determine bacterial migration to and replication within the cLN.

The infection experiments were performed using a mixture of seven *S. Tm* strains, each carrying a unique, 40 base pair long tag in the chromosome [18]. These strains are phenotypically identical to each other and to wild type *S. Tm*. The rationale for using mixed inocula was to reveal the stochasticity of the colonization process: for an appropriate mixing ratio, only some of the strains in the mix arrive in the cLN. The stochastic loss of WITS on their way to the cLN enables us to estimate the rate at which they immigrate. The strains that successfully enter the cLN subsequently increase in numbers. From these numbers, we can infer the growth rate of the bacterial population in the cLN.

Before we present our findings, let us elaborate the advantages of using mixed inocula for studying of the colonization dynamics of the cLN. As we stated above, if we simply measure the bacterial population size in the cLN it is difficult to disentangle immigration from replication. Figure 1 illustrates this point. It shows simulations (based on the mathematical model described below) for a scenario with high immigration and low replication, and an alternative scenario with low immigration and high replication. The parameters are chosen such that the bacterial population sizes in the cLN are approximately equal for both scenarios one day after inoculation. Because the time courses of the bacterial population size in the cLN do not differ dramatically across the two scenarios it is, on the basis of such data, very challenging to determine which of them applies.

In these simulations, the variation of the bacterial population size arises only from the intrinsic stochasticity of bacterial division, clearance (i.e. the bacterial elimination or migration to other organs) and immigration from the gut. In real mice, the distinction between the two scenarios would be blurred even more because there would be larger variation in the time courses of the bacterial population size due to biological differences between mice and experimental sources of error. As a consequence, it is not feasible to distinguish the two scenarios on the basis of measurements of the bacterial population size alone.

With mixed inocula, on the other hand, the distinction between the two scenarios is clear-cut. Assume we inoculate with a mix containing seven WITS at a frequency of 1% and 93% untagged bacteria. In the scenario with low immigration, an individual WITS will fail to colonize the cLN in 37% of the cases. Thus, on average more than half of the WITS will be recovered from the cLN one day after inoculation. If immigration is high, however, WITS will fail to colonize in only 2.5% of the cases, i.e. all WITS will be recovered from the cLN in most animals. Using mixed inocula is therefore a much more sensitive approach to determining immigration and growth rates.

The mathematical model we employed to analyze these infection data is a stochastic birth-death process extended by immigration (see Materials & Methods). It predicts the bacterial population size of each WITS in the cLN as a function of the rate of immigration into the cLN, μ , the rate of replication within the cLN, r , and rate of clearance in the cLN, c . Thus, our model goes beyond simply considering the presence or absence of WITS in the cLN. While the absence of a WITS is equivalent to a population size of 0 CFU, a WITS that is present in the cLN can have any positive population size (1,2,3, ...CFU).

From measurements of the population size of differently tagged bacteria recovered from the lymph node at a given time point, we can estimate the migration rate of bacterial cells from the gut to the cLN, and the net growth rate, $\Delta r = r - c$, of the bacterial population in the cLN using the likelihood we derived for our model (see Materials & Methods). Unfortunately, not all three

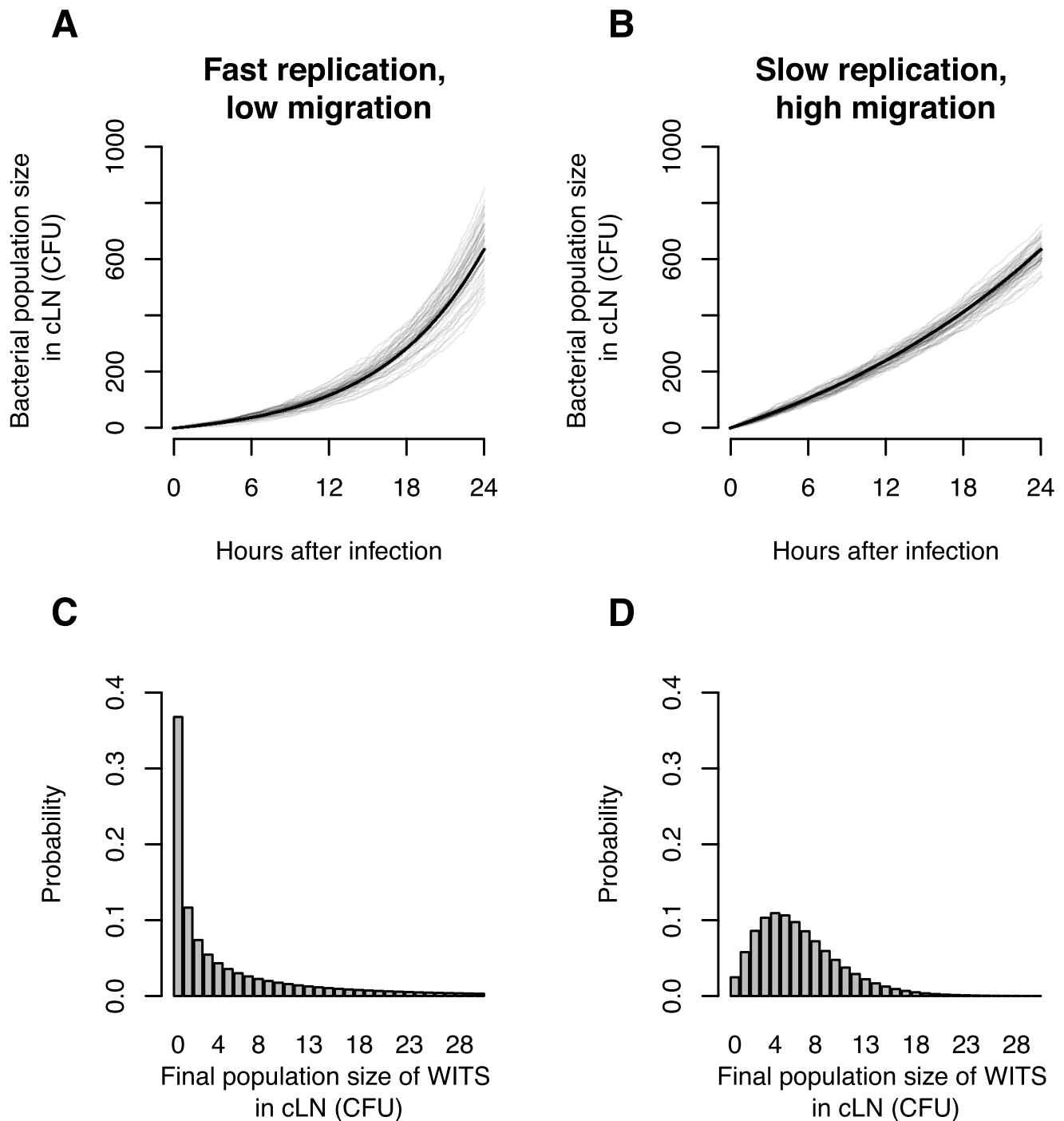


Figure 1. *In silico* analysis demonstrates the value of infection experiments with mixed inocula. **A.** Total bacterial population size in cLN for 50 simulations of a scenario with low migration rate into the cLN (100 bacterial cells per day) and fast net replication therein (doubling time of 5.5 hours). **B.** Total bacterial population size in cLN for the reverse scenario (immigration of 370 bacterial cells per day into the cLN and a doubling time of 16.6 hours). Gray lines indicate the output of individual simulation runs, and the black line is the analytically predicted mean bacterial population size. **C.** and **D.** The probability that WITS attain a specific population size in the cLN 24 hours after infection in the two scenarios. The frequency of a single WITS in the inoculum is assumed to be 1%. While the time courses of the bacterial population size at the top display only subtle differences, the probability distributions on the bottom are clearly distinct for the two scenarios. Thus, using mixed inocula one can disentangle division and immigration much more sensitively than by determination of the total bacterial population size only. doi:10.1371/journal.ppat.1003532.g001

parameters of our model can be estimated independently from our data (see Materials & Methods). We still formulate the mathematical model in terms of the three processes immigration, replication, and clearance, as this is the most intuitive way to conceptualize the

colonization of the cLN. Furthermore, only such a formulation allows us to understand the estimates of the process rates depend on each other (see Materials & Methods). Lastly, clearance and replication can be estimated from alternative experimental setups.

Thus, a model with all three parameters may also be useful for future analysis.

Baseline migration and replication rates

We first conducted experiments in wild type C57BL/6 mice. Eleven mice were inoculated with a mixture of 95% untagged wild type *S. Tm*, and 5% WITS (5×10^7 CFU in total by gavage; see Figure 2A). Each WITS carried one of seven distinct tags. These different strains were represented at equal ratios, i.e. each WITS was represented at a frequency of 0.7% in the inoculum.

Four to six hours after infection the bacteria had reached the large intestine and grew up to a population size of 10^9 . The composition of the bacterial population in the gut of the mice did not differ substantially from that of the inoculum over the course of the experiment (supporting Figure S1). Thus, the bacterial population did not encounter any detectable bottlenecks between the stomach and the gut.

Twenty-four hours after inoculation, the mice were sacrificed to determine the number and composition of bacteria in the cLN (see Figure 2). About 13% of the distinct WITS were lost and could not be recovered from the cLN. The population size of each WITS that successfully migrated into the cLN ranges from 1 to 47 colony forming units (CFU) (see Figure 3A).

From these numbers, we estimated that the net growth rate, Δr , of the bacterial population is $2.82/d$, which corresponds to a doubling time of 5.9 hours (see Table 1). The migration rate of each WITS to the cLN was estimated as $2.13/d$. Extrapolated to the entire bacterial population (i.e. WITS and untagged *S. Tm*), this corresponds to a migration rate of 298 cells per day. Given that the population size in the gut is approximately 10^9 cells, this rate of migration is surprisingly low. It means that one bacterial cell has only a chance of 3×10^{-7} to migrate into the cLN during the first day after inoculation. This step therefore constitutes a major bottleneck for the infection.

Visualizing the agreement between the observed and predicted number of WITS in the cLN is not straight-forward. The reason for this is that our model formalizes migration and division as stochastic processes, and therefore does not make a deterministic prediction on the population size of WITS in the cLN. Rather, our model gives us the probability to observe a certain population size. For example, with the best estimates for our parameters, the predicted probability to observe 1 CFU of a single WITS in the cLN 24 hours after the infection is 0.085. The probability to observe 0 CFU, i.e. not to recover a WITS, is 0.12.

Moreover, the space of potential population sizes (any natural number) is large compared to the number of observations. In the present case, for example, we have measured the population sizes of seven WITS in 11 mice. Thus, we have 77 observations. More than half of these observations are population sizes below 10 CFU, the rest is scattered between 10 and 47. The sparseness of the observations gives rise to seeming discrepancies between the predicted and observed population sizes of WITS in the cLN 24 hours after infection (see Figure 3A).

These difficulties in visualizing the quality of the model fit can be overcome by plotting the cumulative distribution function of predicted and observed population sizes of WITS. The cumulative distribution function describes the fraction of observed or predicted measurements less than or equal to some population size. For example, we mentioned above that more than half of our observations are less than 10 CFU. This can be seen from the cumulative distribution function plotted in Figure 3B: the cumulative distribution function for a population size of 9 CFU is 0.52 and 0.58 for observed and predicted measurements of population sizes, respectively. For high population sizes, the

cumulative distribution function approaches 1. Plotting these cumulative distribution functions shows the good agreement between the observed and predicted population sizes of WITS in the cLN after 24 h of infection (see Figure 3B).

To statistically test for the goodness of fit, we apply a χ^2 test. In order to apply this test we need define intervals of population sizes that contain a minimum of five observations per interval. For most of our datasets, population sizes 0 CFU, 1–5 CFU, 6–20 CFU, and larger than 20 CFU fulfill this criterion. For the fits of our model to the wild type WITS data, this test yields no significant discrepancy between the predicted and observed population sizes of WITS (χ^2 goodness-of-fit test: $X^2 = 0.34$, $df = 3$, $p = 0.95$).

As an independent validation of our model, we can predict the total bacteria population size in the cLN (see Figure 4A). This validation is independent because the data on the total bacterial population sizes in the cLN were not taken into account when estimating the parameters. There is good agreement between the prediction and the observation: with a net growth rate of 2.82 per day and a migration rate of 298 cells per day, our model predicts a population size of, on average, 1667 bacterial cells in the cLN; in comparison, we observed a mean of 1684 cells, ranging from 950 to 2390. This concordance is quite remarkable, and provided evidence that the population parameters inferred from our WITS data analysis can be extrapolated to the entire population.

Impact of inflammation and SPI-1

To investigate the role of inflammation, we compared the infection dynamics of wild type *S. Tm* and a non-invasive mutant *S. Tm* Δ SPI-1 [21]. This mutant has a genetic defect rendering the type three secretion system I (TTSS-1) inactive, and hence does not cause inflammation during the course of our infection experiment [19]. We inoculated eight mice with a mix of 90% untagged, and 10% tagged strains of Δ SPI-1. The tagged fraction contained equal proportions of seven WITS.

For the Δ SPI-1 strain, we estimated a migration rate from the gut to the cLN of 78 cells per day (see Table 1). Thus the migration rate is four times lower than that of wild type *S. Tm*. The reduction of the migration rate is consistent with the key role of the SPI-1 encoded type III secretion system in traversing the gut epithelial barrier, a key step for reaching the cLN [22,23]. Compared to wild type *S. Tm* the net replication rate of Δ SPI-1 is increased from 2.82 per day to 3.68 per day. This corresponds to a decrease in the population's net doubling time from 5.9 to 4.5 hours.

The black and grey lines in Figure 3C show the cumulative distribution functions for observed and predicted WITS population sizes in the cLN. Again, there is an excellent agreement between data and model predictions (χ^2 goodness-of-fit test: $X^2 = 1.08$, $df = 3$, $p = 0.78$). With the estimated parameters, our model can again be validated by predicting the total bacterial population size in the cLN. There is very good agreement with the experimental data, even though these measurements were not used for the parameter estimation: the model predicts an average of 819 bacterial cells in the cLN one day after inoculation, while we measured 881 cell on average, ranging from 290 to 1640 (see Figure 4B).

To investigate the cause of these differences in the immigration and net replication rates, we conducted experiments in which the inoculum consisted of wild type *S. Tm* and Δ SPI-1. On the one hand, we used inocula, in which the large majority of the inoculum consisted of wild type *S. Tm* but the WITS lacked SPI-1. We have shown earlier that this type of infection elicits gut inflammation [24]. On the other hand, using inocula mainly consisting of

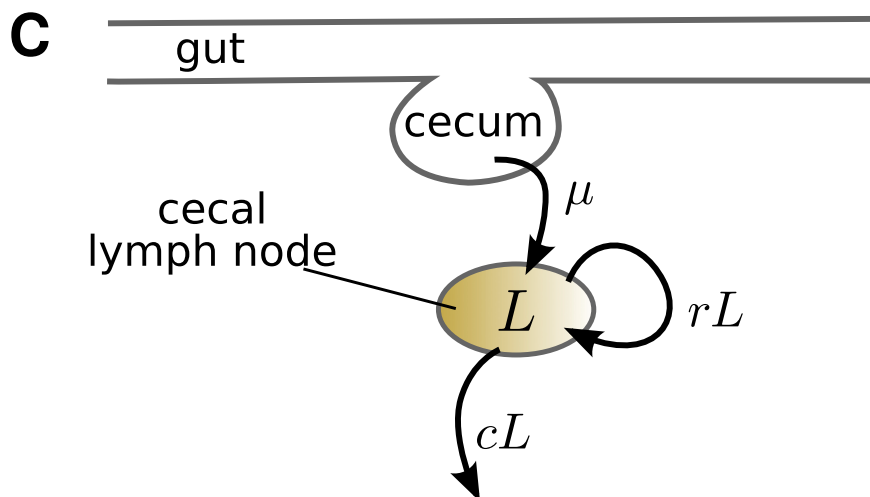
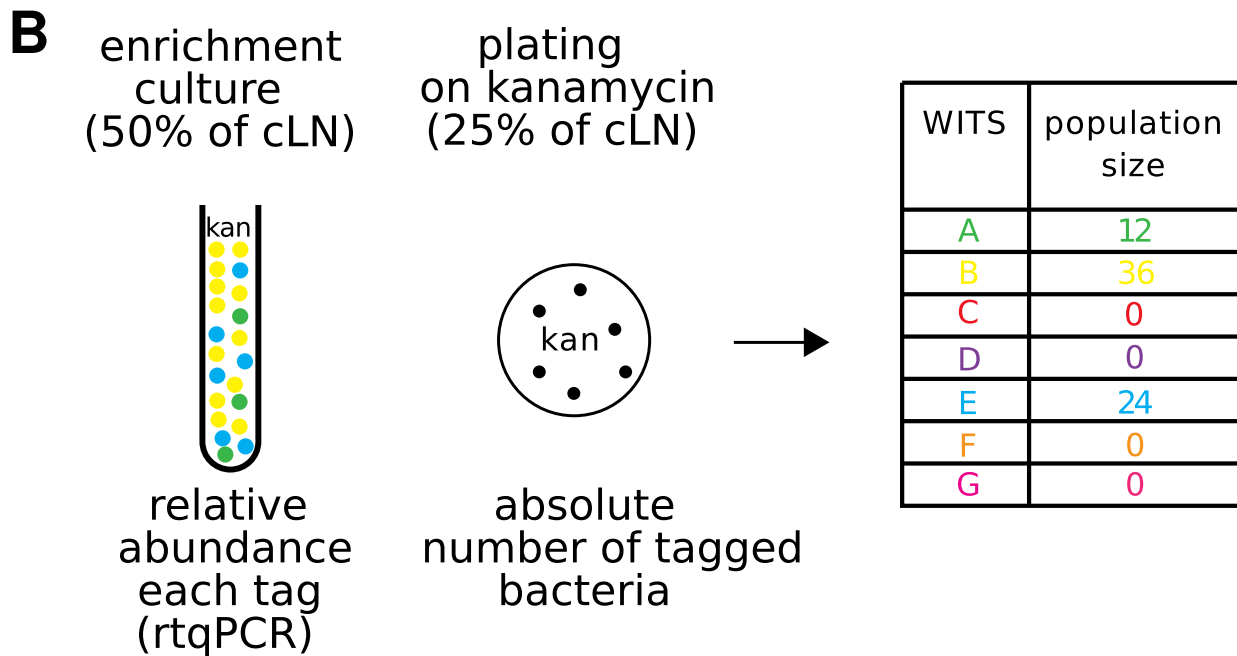
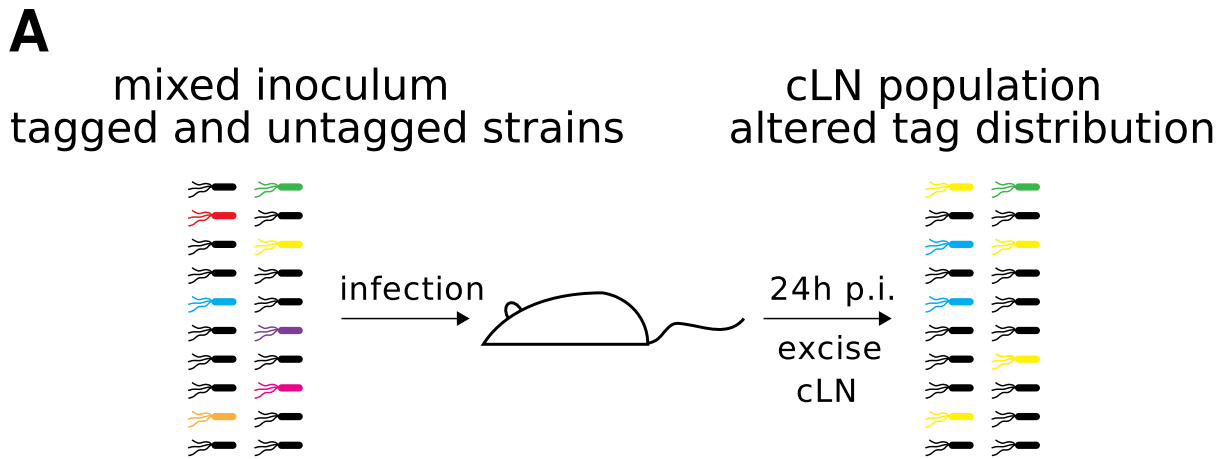


Figure 2. Experimental protocol for infections with mixed inocula. A. A mixture of all 7 WITS at equal ratios was diluted with a 20-fold excess of untagged *S. Tm* and used as an oral inoculum. The inoculum was plated to control for correct ratio of tagged to untagged bacteria. After 24 hours, the cLN was sterily removed and smashed. 50% of the cLN was inoculated into a kanamycin containing overnight culture, 25% each were plated either on a streptomycin or kanamycin containing McConkey agar plates. **B.** Typical dataset: genomic DNA of overnight culture was isolated and subjected to rtqPCR (see Materials & Methods). To obtain the population size of bacteria carrying a specific tag, the relative rtqPCR signal was multiplied with the population size of WITS in the cLN, which we determined by plating on the kanamycin plate. **C.** Diagrammatic representation of our mathematical model. The model describes the population size, L , of bacteria in the cecal lymph node. It incorporates the migration of bacteria from the cecum to the cecal lymph node at a rate μ , and the replication and clearance of bacteria in the lymph node at rates rL and cL , respectively. These processes are assumed to be stochastic.
doi:10.1371/journal.ppat.1003532.g002

Δ SPI-1 while the wild type *S. Tm* carried the tag, we could analyze the population of wild type *S. Tm* in a healthy, non-inflamed gut environment [24].

When the large majority of the inoculum consisted of wild type *S. Tm*, i.e. inflammation was induced, the population of WITS that lacked SPI-1 increased with a net doubling time of 6.5 hours

(see Table 1). This estimate is similar to the net doubling time of wild type *S. Tm* (5.9 hours — see Table 1, top row), and significantly larger than the net doubling time of Δ SPI-1 without inflammation (4.5 hours — see Table 1, second row). The migration rate estimate of Δ SPI-1 to the cLN was twice as high as without inflammation: when extrapolated to the entire

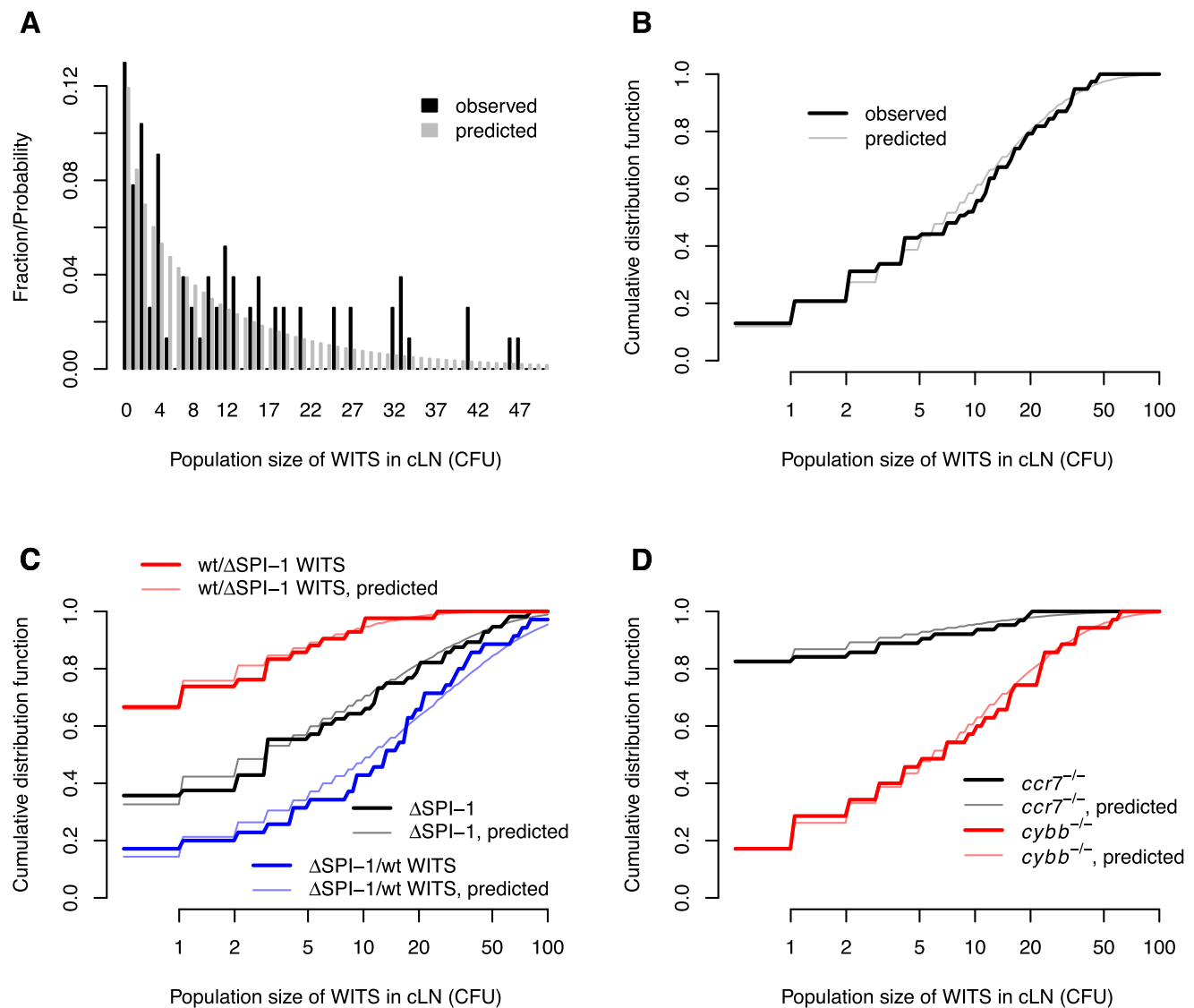


Figure 3. Comparison between the observed and predicted population sizes of the WITS. A. Comparison of observed and predicted wild type WITS population size distributions in wild type mice. **B.** The same comparison, but cumulative distribution functions of the WITS population sizes are shown. **C.** Comparison of observed and predicted WITS population size distributions in wild type mice for experiments involving Δ SPI-1. **D.** Comparison of observed and predicted WITS population size distributions in *ccr7*^{-/-} and *cybb*^{-/-} mice. The model predictions are based on the maximum likelihood estimates in Table 1.
doi:10.1371/journal.ppat.1003532.g003

Table 1. Estimates of the migration rate of bacteria into the cLN, their net replication rate, Δr , and the corresponding doubling time.

| <i>Salmonella</i> strain | Mouse genotype | migration rate to cLN (per day) | Δr (per day) | doubling time (hours) |
|---------------------------------------|----------------------------|---------------------------------|----------------------|-----------------------|
| wild type | wild type | 298 (242–391) | 2.82 (2.46–3.07) | 5.9 (5.4–6.8) |
| Δ SPI–1 | wild type | 78 (50–108) | 3.68 (3.15–4.09) | 4.5 (4.1–5.3) |
| wild type, Δ SPI–1 WITS (50:1) | wild type | 146 (65–242)* | 2.57 (1.59–3.20)* | 6.5 (5.2–10.5)* |
| Δ SPI–1, wild type WITS (20:1) | wild type | 272 (183–412)* | 3.94 (3.04–4.63)* | 4.2 (3.6–5.5)* |
| wild type | <i>ccr7</i> ^{-/-} | 28 (11–70) | 3.31 (2.96–4.19) | 5.0 (4.0–5.6) |
| wild type | <i>cybb</i> ^{-/-} | 1241 (863–2050) | 3.13 (2.51–3.59) | 5.3 (4.6–6.6) |

95% confidence intervals are given in brackets.

*values calculated for the WITS and extrapolated to the entire bacterial population.

doi:10.1371/journal.ppat.1003532.t001

population, 146 and 72 cells migrated to the cLN per day with and without inflammation, respectively. But this difference was not statistically significant.

In the converse experiment, in which the inoculum consisted mainly of Δ SPI–1 but the WITS expressed SPI-1, we estimated almost the same immigration rate as for wild type *S. Tm* (see Table 1, top row), and the same doubling time as for Δ SPI–1 (see Table 1, second row).

The fits of the model to these two datasets are shown in Figure 3C. Both fits passed a χ^2 goodness of fit test (wild type, Δ SPI–1 WITS: $X^2 = 0.14$, $df = 2$, $p = 0.93$; Δ SPI–1, wild type WITS: $X^2 = 1.01$, $df = 3$, $p = 0.80$).

Taken together, these experiments show that inflammation decreases the net replication rate in the cLN. The most likely explanation for this finding is an increase in bacterial clearance by immunity in the cLN. But inflammation does not significantly affect the migration between gut and cLN.

Impact of host innate immunity

There are a number of important players in the innate immune response against *S. Tm*, including dendritic cells and phagocytes producing reactive oxygen species that are toxic to the pathogen. The general function of dendritic cells is to sample antigen, to

present it to T helper cells, and thus to initiate the adaptive immune response. In *S. Tm* infections dendritic cells take up bacterial cells when they sample the gut, and subsequently carry them into the lymph node [25–27]. Oxygen-derived compounds are produced in phagocytes, such as neutrophils, and, to a lesser extent, in macrophages, after they have engulfed bacteria. These compounds are thought to kill the bacteria within the phagocytes, and, as a result, to reduce pathogen loads in the gut mucosa and other infected sites [24]. In summary, phagocytes have profound effects on the infection process. However, their function in controlling pathogen population dynamics had remained poorly understood.

To assess the role of dendritic cells for the early colonization dynamics with *S. Tm* we conducted infection experiments in mice lacking CCR7, in which dendritic cell movement is impaired [28]. In these *ccr7*^{-/-} mice, we find the bacterial migration rate to the cLN to be more than 10-fold lower than in wild type animals: only 28 *S. Tm* cells migrate from the gut to the cLN per day (see Table 1). The few *S. Tm* cells that enter the cLN have a slightly, but significantly higher net replication rate than in wild type mice. As for the Δ SPI–1, this is more likely due to reduced clearance, rather than an increased rate of division.

The fit of our model to the experimental data collected in *ccr7*^{-/-} mice passes the visual and statistical test of goodness. The

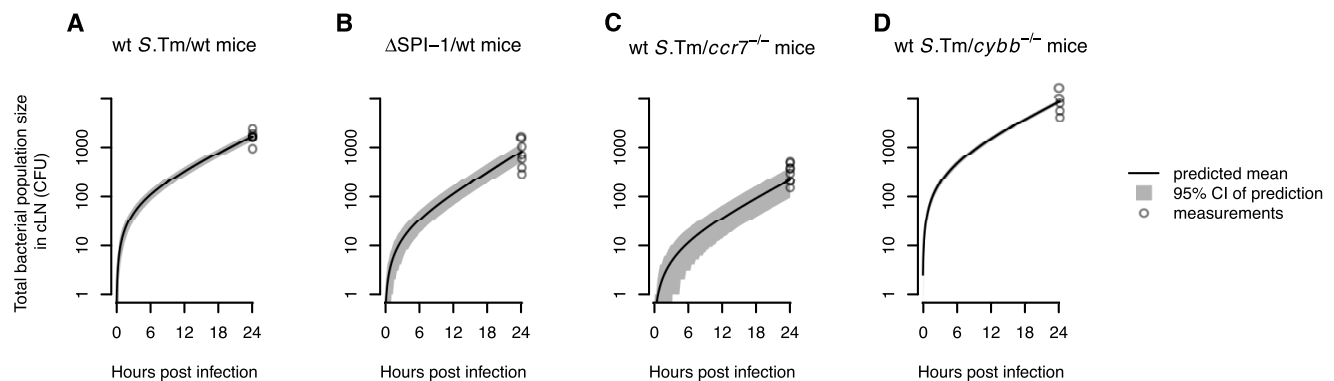


Figure 4. The WITS-based model predictions are consistent with the total bacterial population size measured in the cLN. Model predictions of the mean total bacterial population size in the cLN over time are shown for the different experiments. Gray areas show the 95% confidence intervals for the model predictions. **A.** Wild type mice infected with wild type *S. Tm*. **B.** Wild type mice infected with Δ SPI–1. **C.** *ccr7*^{-/-} mice infected with wild type *S. Tm*. **D.** *cybb*^{-/-} mice infected with wild type *S. Tm*. For *cybb*^{-/-} mice the confidence intervals are very narrow and therefore hardly visible. In all plots, circles denote the total bacterial population sizes observed in the cLN 24 hours after infection.

doi:10.1371/journal.ppat.1003532.g004

observed and predicted cumulative distributions of WITS population sizes coincide (see the black and gray lines in Figure 3D, respectively). The fit of our model also passed a χ^2 goodness of fit test ($\chi^2=0.66$, $df=2$, $p=0.72$). There is also good agreement between the predicted and observed the total bacterial population size in the cLN: the model predicts 220 bacterial cells, while we measured bacterial population sizes ranging from 150 to 507 cells (see Figure 4C).

The role of toxic oxygen derivatives was assessed in *cybb*^{-/-} mice that have a deletion in the *p91phox* subunit of nicotinamide adenine dinucleotide phosphate oxidase, a key enzyme in the generation of reactive oxygen species. In these mice, the migration rates were four times higher than in normal mice, while there was no difference in net replication rate (see Table 1). As for all the other experiments, we observed a good agreement between model predictions and the experimental data (χ^2 goodness-of-fit test: $\chi^2=0.99$, $df=3$, $p=0.80$; also see Figure 3D and Figure 4D).

Discussion

In this study, we estimated dynamical parameters that characterize the colonization of the cecal lymph node of mice by *Salmonella* Typhimurium, the pathogen's first step to systemic infection. Our approach relied on infection with mixed inocula, which augmented the stochasticity of the processes involved in colonization. Exploiting this stochasticity, we could derive the rate at which the bacterial immigrate from the gut, and the net growth rate of the bacteria population in the cLN.

Performing our analysis with different bacterial strains and knock-out mice allowed us to determine the impact of various bacterial virulence factors and elements of the host's immune defense on the colonization dynamics. The inflammatory response induced by TTSS-1 was found to significantly reduce the net replication rate of bacteria in the cLN but had no significant effect on the migration rate to the cLN.

Our analysis in *ccr7*^{-/-} mice showed a strong and statistically significant reduction in migration to the cLN from 298 to 28 cells per day. These mice are commonly applied to assess the influence of impaired dendritic cell migration on infections and the elicitation of immune responses. Our result therefore strongly suggest that that dendritic cells play a key role in the migration of *S. Tm* from the gut to the cLN. This would be in line with previous work [25–27,29,30]. Nevertheless, since *ccr7*^{-/-} mice have a complex phenotype, alternative explanations cannot be dismissed completely.

In *cybb*^{-/-} mice, which lack reactive oxygen species, migration was dramatically increased, while the net replication rate remained unchanged. The parameter estimates are in line with unaltered *S. Tm* growth within *cybb*^{-/-} macrophages [31] and increased pathogen population sizes in the cecal lamina propria (see [24] and data not shown). These findings indicate that elimination of bacteria on their way from the gut lumen into the cLN, e.g. in the lamina propria or the transporting phagocytes, is the key factor explaining the increased migration rates to the cLN in *cybb*^{-/-} mice.

What are the limitations of our approach? Our current mathematical model is only a crude reflection of the biological realities involved in the colonization of the cecal lymph node by *S. Tm*. As any modeling study, we had to make simplifying assumptions. First, we assumed that migration rate is constant over time. This assumption is justified for migration because the population size of *S. Tm* in the gut — the source for the migration to the cLN — remains approximately constant over the period of

observation. We also assumed that the replication of bacteria in the cLN occurs at a constant rate, which is a valid assumption if the population sizes do not exceed the carrying capacity of the compartment. In our case, the bacteria population in the cLN reaches about 1000 CFU within a day, which is approximately fifty fold lower than the carrying capacity of the cLN [22].

On a more subtle point, our mathematical formulation of replication and clearance implicitly assume exponentially distributed inter-division times and lifespans of bacterial cells. More realistic distributions will certainly affect the colonization dynamics. However, a reliable determination of these distributions will have to rely on individual cell measurements that were not available in this study. Extending our model by more realistic distributions of inter-division times and lifespans will be an important topic for future work.

Furthermore, our model does not explicitly account for the fact that the bacteria replicate within cells. Recent studies have started to unravel the dynamics of *Salmonella* replication within the cells of the host [32,33]. In the future, these models will have to be combined with the mathematical description of the colonization of the host presented in this paper. Lastly, our current mathematical model neglects the detailed molecular mechanisms involved in the migration through the lamina propria.

As a consequence of the simplifying assumption we made, our model parameters have to be interpreted with care as they comprise multiple processes. The migration rate, for example, measures the effective flux of bacteria between gut and cLN. It comprises the aspects related to the movement or transport of the bacteria between these two compartments, such as bacterial penetration of the epithelial barrier, the cells they use as vehicles, their migratory speed and their sense of direction. This is important for interpreting the increase in migration rate in *cybb*^{-/-} mice. Because these mice lack reactive oxygen defenses, the higher migration rate is most likely due to a decrease in killing of bacteria on their way to the cLN, and not to faster migration or transport. Similarly an increase in the net replication rate — as we found for Δ SPI-1 and in *ccr7*^{-/-} mice — can be due to faster division as well as lower rates of clearance.

At the current state of research, the main reason in favor of a simple mathematical model is to avoid over-parameterization. The higher the number of model parameters, the more difficult it is to estimate each parameter reliably. Even with three parameters, we encountered the problem that division and clearance rates were not independently identifiable. Thus, adding more complexity to the mathematical model will have to go hand in hand with experiments that provide the data necessary for reliable parameter estimation. This will be an important topic for future work.

There is a long history in microbiology of using mixed inocula to elucidate colonization dynamics of bacterial pathogens. The earliest studies on this topic [12,13], used various strains of *Salmonella* to investigate if bacterial cells cooperated during the colonization of mice. The conclusion of these studies was that each cell had the same probability to colonize, a scenario called the *hypothesis of independent action* [34,35]. Also our mathematical model conforms to this hypothesis. Quantitative conclusions about migration and replication were not drawn in these studies.

Later Moxon and Murphy [14] adopted the same approach for *Haemophilus influenzae*. They went beyond the first studies [12,13] by sampling bacteria from different compartments. In addition to confirming the hypothesis of independent action, Moxon and Murphy could elucidate the colonization pathway of the pathogen. But again, as no replication and migration parameters were estimated, the conclusions of this study with regard to the colonization dynamics remained qualitative.

Margolis & Levin [16] recently investigated if bacterial evolution is required for invasive infection in the *H. influenzae* system — a hypothesis put forward in [36]. They concluded that invasion has a strong stochastic element, and the probability that a bacterial cell causes invasive infection is very low. They also find evidence for within-host evolution towards higher invasiveness. According to Margolis & Levin, the low probability of invasion and occasional evolution of invasive mutants provides an explanation of the monoclonality of invasive infections.

Our data suggest that within-host evolution towards higher invasiveness is unlikely in *S. Tm* infections. If particular mutations were necessary for the migration to the lymph node they would arise more frequently in the untagged than in the tagged population because the untagged population is at least 10 times larger in our experiments. In that case, we would be unable to extrapolate the migration rate of the WITS to that of the total bacterial population. However, the parameter estimates we obtain from the WITS allow us to predict the total bacterial population sizes in the cLN in most of our experiments (see Figure 4). Additionally, the particular migration rate we estimate (300 cells per day) implies that the systemic population of *S. Tm* is not going to be monoclonal.

More recently, WITS have been used to elucidate colonization pathways of *Yersinia pseudotuberculosis* gut infection [17] and systemic salmonellosis [18]. The main advantage of WITS over the strains used in the early studies [12–14] is that many distinct strains can be constructed, and that the tag is less likely to affect the phenotype, in particular the replication rate. Only in the study by Grant et al [18] estimates for parameters that characterize the within-host dynamics were obtained.

There are important differences between that previous study and our work. First, Grant et al. studied bacterial spread following intravenous infection of mice. In their model system, bacteria migrate from the blood into the spleen and the liver after inoculation. The intestine, however, is not infected efficiently and is not inflamed [22]. This system is therefore mainly of value for the study of the systemic spread of the typhoid fever-like infection. But since intravenous inoculation circumvents the epithelial barrier of the gut, the model system of Grant et al. is of limited use for the study of the first steps of the natural infection, i.e. after orogastric exposure.

Second, the estimation of the dynamical parameters in Grant et al. centered on the presence of WITS and the total bacterial population size in different anatomical compartments, and did not include information on the population size of each WITS. Their mathematical models also featured many more parameters than ours because bacterial spread and replication in multiple compartment had to be described. As a consequence, confidence intervals could not be determined for all model parameters. Without confidence intervals, differences in parameters between bacterial strains or mice genotypes cannot be established formally.

Our current approach allowed estimating key parameters of the within-host dynamics during the early phase of the diarrheal *S. Typhimurium* infection. While estimates of the dynamical parameters that characterize the colonization of the cLN are more difficult to obtain than standard readouts, such as pathogen load at some time after infection, they provide more relevant information: they tell us what happens with the bacteria over time, and thereby supply more than just snapshots of the system. Understanding the processes that the bacteria undergo is most relevant for the design of vaccines and treatment.

Materials and Methods

Experiments

Ethics statement. All animal experiments were approved by the authorities (Kantonales Veterinäramt Zürich, license: 223/2010) and performed according to local guidelines (TschV, Zürich) and the Swiss animal protection law (TschG).

Bacterial strains and growth conditions. The wild type strain SB300 (*S. enterica* subspecies 1 serovar Typhimurium) and the avirulent mutant Δ SPI–1 (Δ invG) are SL1344 derivatives and have been described previously [21,37–39]. Wild type isogenic tagged strains (WITS) were previously described by A.J. Grant [18]. Tags were transduced into avirulent strains using p22 phage transduction and subsequent selection on kanamycin. For infection experiments, the bacteria were grown over night in LB broth (containing 0.3 M NaCl), sub-cultured for 4 hours and suspended in cold PBS as described previously [38].

Wild type isogenic tagged strain quantification. Streptomycin pre-treated mice were infected according to our standard infection protocol [19] with a uniform mixture of 7 isogenic tagged strains [18]. Tagged strains were diluted with an excess of untagged *S. Tm*. The ratios of tagged to untagged strains were 1:20 in most cases except for the experiments with Δ SPI–1, the experiments with untagged wild type *S. Tm* and Δ SPI–1 WITS, and the experiments in *cybb*^{-/-} mice that were conducted with a ration of 1:10, 1:50, and 1:100, respectively. Mice were killed by cervical dislocation and the cecal lymph node was aseptically removed and homogenized in 500 μ l of ice-cold PBS (0.5% Tergitol, 0.5% bovine serum albumin) by using a Potter homogenizer. 250 μ l of the lymph node homogenate was inoculated into an LB overnight culture containing 50 μ g/ml Kanamycin to enrich for tagged *Salmonella* spp and 150 μ l were plated on MacConkey agar plates to determine colony forming units (CFU). Chromosomal DNA from enrichment cultures was isolated using the QIAamp DNA Mini Kit (Qiagen, Cat. No. 51306) and subjected to rtqPCR using the FastStart Universal SYBR Green Master (Rox) (Roche, 13206900) mix with primers and temperature profiles described in [18]. The ratio of the WITS was multiplied with the number of CFUs recovered to determine the population size of each tagged strain in the cecal lymph node. The culturing and rtqPCR set does not bias our measure of the population size of tagged bacteria (see Figure S2).

Mouse experiments. Homozygous B6.129P2(C)-Ccr7tm1Rfor/J [28], homozygous B6.129S-Cybbtm1Din/J (C57BL/6 background; [40]) and wild type C57BL/6 mice were bred and kept specified pathogen free in individually ventilated cages (RCHCL, ETH Zürich). All animal experiments were approved (licences 201/2007, 223/2010, Kantonales Veterinäramt Zürich) and performed as legally required. Streptomycin pretreated mice (20 mg/animal) were infected by gavage (5×10^7 CFU; [19,26]). Live bacterial loads (CFU) in cLN, spleen, liver, and cecal content were determined by plating [26].

Mathematical modelling and statistical analysis

Model definition. To model the colonization of mice by *S. Tm*, we developed a simple stochastic model that describes the immigration of bacterial cells into the cecal lymph node (cLN) and their replication and clearance in that compartment.

The model assumes that *S. Tm* migrate from the gut to the cLN at a constant rate μ . Once arrived in the cLN, a bacterial cell can divide at rate rL or be cleared at rate cL . Hereby, L denotes the bacterial population size in the cLN. (Figure 2C shows a diagram of our mathematical model.) To keep the exposition of our model as general as possible we are, at this stage, refraining from defining

which exact bacterial population the variable L refers to. It can and will refer either to the population of WITS carrying a unique tag (when we analyze the experimental data and estimate model parameters), or to the total $S. Tm$ population in the cLN (when we simulate the colonization dynamics).

To be able to describe the event that the cLN is not colonized by WITS, we formulate the model as a continuous-time Markov process. This process has the following transition probabilities:

$$\begin{aligned} Pr(L(t+h)=k+1|L(t)=k) &= \mu h + rL h + o(h), \quad k=0,1,2, \dots \\ Pr(L(t+h)=k|L(t)=k+1) &= cL h + o(h) \\ Pr(L(t+h)=k+j|L(t)=k) &= o(h), \quad |j|>1 \end{aligned} \tag{1}$$

Hereby, k is a non-negative integer, $k=0,1,2, \dots$, and j is an integer with $|j|>1$. This process extends the well-known birth-death process by immigration [41].

These transition probabilities lead to the following master equations for the state probabilities, $p_k(t) = Pr(L(t)=k)$:

$$\begin{aligned} dp_0/dt &= -\mu p_0 + c p_1 \\ dp_1/dt &= +\mu p_0 + (-\mu - r - c) p_1 + 2c p_2 \\ dp_2/dt &= +(\mu + r) p_1 + (-\mu - 2r - 2c) p_2 + 3c p_3 \\ &\vdots \\ dp_k/dt &= +(\mu + (k-1)r) p_{k-1} + (-\mu - kr - kc) p_k + (k+1)c p_{k+1} \\ &\vdots \end{aligned} \tag{2}$$

Initially, we have no WITS in the cLN, which is equivalent to the initial conditions $p_0(0) = 1$ and $p_k(0) = 0, k = 1, 2, \dots$

Analogously to the birth-death process, we can derive the probability generating function that is defined as $f(s,t) = \sum_{k=0}^{\infty} p_k s^k$. This function comprehensively characterizes the distribution of the bacterial population size in the cLN at time t . Substituting the master equations 2 into the definition of $f(s,t)$ leads to a partial differential equation for f that can be solved using the method of characteristics [42]. For the initial condition $f(s,t=0) = 1$, which corresponds to an initially empty lymph node ($p_0(0) = 1$ and $p_k(0) = 0, k = 1, 2, \dots$), we thus obtain:

$$f(s,t) = \left[\frac{r-c}{r s (1 - e^{(r-c)t}) + r e^{(r-c)t} - c} \right]^{\frac{\mu}{r}} \tag{3}$$

From the probability generating function we can obtain the state probabilities $p_k(t)$ in closed form by using the relation $(\partial_s^k f)(0,t) = k! p_k(t)$. This yields:

$$p_k(t) = \left[\frac{r-c}{r e^{(r-c)t} - c} \right]^{\frac{\mu}{r}} \left[\frac{r(1 - e^{(r-c)t})}{r e^{(r-c)t} - c} \right]^k \prod_{j=1}^k \left(1 + \frac{\mu}{r} - \frac{1}{j} \right) \tag{4}$$

Figure S3 shows the time courses of p_k for $k=0,1,2, \dots, 30$. We can also obtain the mean bacterial population as a function of the time t , $\bar{L}(t)$, using the relation $\bar{L}(t) = \partial_s f(1,t)$:

$$\bar{L}(t) = \frac{\mu(e^{(r-c)t} - 1)}{r - c} \tag{5}$$

Maximum likelihood parameter estimation. Assume we conduct an experiment involving M mice, each infected with an inoculum that contains a small fraction of WITS. Assume further

we have seven WITS in the inoculum, and that they are present at the same frequency in the gut. Because each WITS is present at the same frequency in the gut we assume that their rate of migration into the cLN is the same. We further assume that there are no differences in the migration, replication and clearance rates between mice. We denote the universal migration rate of a WITS by μ_W .

One day after inoculation, the population sizes of WITS are determined. We denote this population size as k_{mi} , where the index $m = 1, \dots, M$ indicates the mouse in which the measure was taken, and $i = 1, \dots, 7$ the specific WITS, the population size of which was determined. The log-likelihood for the data k_{mi} is:

$$\ell(r,c,\mu_W|k_{mi}) = \sum_{m=1}^M \sum_{i=1}^7 \ln p_{k_{mi}}(1d) \tag{6}$$

$$= \sum_{m=1}^M \sum_{i=1}^7 \left[\alpha \ln \zeta + k_{mi} \ln(1 - \zeta) + \sum_{j=0}^{k_{mi}} \ln \left(1 + \frac{\alpha - 1}{j} \right) \right] \tag{7}$$

Hereby $\alpha = \frac{\mu_W}{r}$ and $\zeta = \frac{r-c}{r e^{(r-c)t} - c}$.

Maximizing this expression for the log-likelihood allows us to obtain best estimates for the parameters of our model from experimental data on the population sizes of each WITS in each mouse, k_{mi} . Because the expression for the log-likelihood, ℓ , in Equation 7 depends only on the composite parameters α and ζ , it is effectively a function of two parameters only. Thus, r , c , and μ_W are not independently identifiable from our experimental data.

Since it is impossible to estimate all three parameters of our model, we set the clearance rate constant of bacterial cells in the cLN $c=0$, and estimated the migration rate μ_W and the replication rate constant r . Figure S4 shows the likelihoods as functions of r and μ_W for the experiments with different $S. Tm$ strains and mice genotypes. It is clear that the likelihood functions are well behaved and that there is only one maximum in the biologically relevant parameter range.

If we set c to a value larger than zero, the maximum likelihood estimate of r increases linearly with a slope slightly less than one (see Figure S5A). Because of this we can interpret the estimate of r assuming $c=0$ as the net growth rate, $\Delta r = r - c$. The estimate of μ_W also increases with the assumed value of c , but with a slope closer to zero (see Figure S5B).

From our estimates of μ_W we calculate the migration rate, μ_T , of the total bacterial population — tagged and untagged — from the gut to the cLN by dividing the estimate for a WITS by its frequency, ω : $\mu_T = \mu_W / \omega$. From our estimates of Δr (per day) we calculate a doubling time (in hours) of the bacterial population in the cLN as $24 \times \ln(2) / \Delta r$. The estimates we thus obtained for μ_T , Δr , and the corresponding doubling times are given in Table 1.

Assessment of the goodness of fit. The quality of the fits were assessed with a χ^2 goodness of fit test [43]. To apply this test, one needs to combine population sizes into bins, in which one has more than five observation. For most of our datasets, we defined the following bins for the population sizes of WITS in the cLN: 0 CFU, 1–5 CFU, 6–20 CFU, and more than 20 CFU. We observed fewer and generally lower population sizes of WITS in the experiments involving untagged wild type $S. Tm$ mixed with $\Delta SPI-1$ WITS and the experiments in $ccr7^{-/-}$ mice. To assess the goodness of fit of the data from these experiments, we therefore used the following bins: 0 CFU, 1–3 CFU, and more than 3 CFU.

The goodness of fit test compares the number of observations in the bins to the number of observations predicted by the birth-death-immigration model with the maximum likelihood parameter estimates. The null hypothesis of this test is that there is no significant discrepancy between observations and model prediction. This null hypothesis was not rejected for any of the datasets we analyzed.

Implementation. All the probability generating functions and likelihoods described here were implemented in the R language of statistical computing [44]. To obtain the maximum likelihood estimates, we used the R-function `optim()`. Confidence intervals for the estimates were obtained with a bootstrap routine from 200 replicates. Goodness of fit tests were conducted using the function `chisq.test()` after the data and the prediction have been binned into the intervals mentioned above. To simulate the process as shown in Figure 4, we used the R-package `GillespieSSA` [45].

Supporting Information

Figure S1 Relative frequency of each WITS in the cecum 24 hours after infection. Measurements for three representative mice are shown. All WITS strains are present at approximately equal frequencies.

(PDF)

Figure S2 WITS at various dilutions can be detected with our protocol that involves overnight culture and rtqPCR. There is no bias against detecting WITS at low frequencies.

(PDF)

References

- Haase AT (2005) Perils of mucosal front lines for HIV and SIV and their hosts. *Nat Rev Immunol* 5: 783–92.
- Shankarappa R, Margolick JB, Gange SJ, Rodrigo AG, Upchurch D, et al. (1999) Consistent viral evolutionary changes associated with the progression of human immunodeficiency virus type 1 infection. *J Virol* 73: 10489–502.
- Keele BF, Giorgi EE, Salazar-Gonzalez JF, Decker JM, Pham KT, et al. (2008) Identification and characterization of transmitted and early founder virus envelopes in primary HIV-1 infection. *Proc Natl Acad Sci U S A* 105: 7552–7.
- Schmitz JE, Kuroda MJ, Santra S, Sasseville VG, Simon MA, et al. (1999) Control of viremia in simian immunodeficiency virus infection by CD8(+) lymphocytes. *Science* 283: 857–860.
- Regoes RR, Antia R, Garber DA, Silvestri G, Feinberg MB, et al. (2004) Roles of target cells and virus-specific cellular immunity in primary simian immunodeficiency virus infection. *J Virol* 78: 4866–4875.
- Fernandez CS, Stratov I, De Rose R, Walsh K, Dale CJ, et al. (2005) Rapid viral escape at an immunodominant simian-human immunodeficiency virus cytotoxic T-lymphocyte epitope exacts a dramatic fitness cost. *J Virol* 79: 5721–31.
- Mandl JN, Regoes RR, Garber DA, Feinberg MB (2007) Estimating the effectiveness of SIV specific CD8+ T cells from the dynamics of viral immune escape. *J Virol* 81: 11982–11991.
- Goonetilleke N, Liu MKP, Salazar-Gonzalez JF, Ferrari G, Giorgi E, et al. (2009) The first T cell response to transmitted/founder virus contributes to the control of acute viremia in HIV-1 infection. *J Exp Med* 206: 1253–72.
- Lay MD, Petravic J, Gordon SN, Engram J, Silvestri G, et al. (2009) Is the gut the major source of virus in early simian immunodeficiency virus infection? *J Virol* 83: 7517–23.
- Baccam P, Beauchemin C, Macken CA, Hayden FG, Perelson AS (2006) Kinetics of influenza A virus infection in humans. *J Virol* 80: 7590–9.
- Bull RA, Luciani F, McElroy K, Gaudieri S, Pham ST, et al. (2011) Sequential bottlenecks drive viral evolution in early acute hepatitis C virus infection. *PLoS Pathog* 7: e1002243.
- Meynell GG (1957) The applicability of the hypothesis of independent action to fatal infections in mice given *Salmonella typhimurium* by mouth. *J Gen Microbiol* 16: 396–404.
- Meynell GG, Stocker BA (1957) Some hypotheses on the aetiology of fatal infections in partially resistant hosts and their application to mice challenged with *Salmonella paratyphi-B* or *Salmonella typhimurium* by intraperitoneal injection. *J Gen Microbiol* 16: 38–58.
- Moxon ER, Murphy PA (1978) *Haemophilus influenzae* bacteremia and meningitis resulting from survival of a single organism. *Proc Natl Acad Sci USA* 75: 1534–6.
- Levin BR, Lipsitch M, Bonhoeffer S (1999) Population biology, evolution, and infectious disease: convergence and synthesis. *Science* 283: 806–9.
- Margolis E, Levin BR (2007) Within-host evolution for the invasiveness of commensal bacteria: an experimental study of bacteremias resulting from *Haemophilus influenzae* nasal carriage. *J Infect Dis* 196: 1068–75.
- Barnes PD, Bergman MA, Meccas J, Isberg RR (2006) *Yersinia pseudotuberculosis* disseminates directly from a replicating bacterial pool in the intestine. *J Exp Med* 203: 1591–601.
- Grant AJ, Restif O, McKinley TJ, Sheppard M, Maskell DJ, et al. (2008) Modelling within-host spatiotemporal dynamics of invasive bacterial disease. *PLoS Biol* 6: e74.
- Barthel M, Hapfelmeier S, Quintanilla-Martinez L, Kremer M, Rohde M, et al. (2003) Pretreatment of mice with streptomycin provides a *Salmonella enterica* serovar Typhimurium colitis model that allows analysis of both pathogen and host. *Infect Immun* 71: 2839–58.
- Kaiser P, Diard M, Stecher B, Hardt WD (2012) The streptomycin mouse model for *Salmonella* diarrhea: functional analysis of the microbiota, the pathogen's virulence factors, and the host's mucosal immune response. *Immunol Rev* 245: 56–83.
- Kaniga K, Bossio JC, Galán JE (1994) The *Salmonella typhimurium* invasion genes *invF* and *invG* encode homologues of the AraC and PulD family of proteins. *Mol Microbiol* 13: 555–68.
- Hapfelmeier S, Stecher B, Barthel M, Kremer M, Müller AJ, et al. (2005) The *Salmonella* pathogenicity island (SPI)-2 and SPI-1 type III secretion systems allow *Salmonella* serovar typhimurium to trigger colitis via MyD88-dependent and MyD88-independent mechanisms. *J Immunol* 174: 1675–85.
- Martinoli C, Chiavelli A, Rescigno M (2007) Entry route of *Salmonella typhimurium* directs the type of induced immune response. *Immunity* 27: 975–84.
- Ackermann M, Stecher B, Freed NE, Songhet P, Hardt WD, et al. (2008) Self-destructive cooperation mediated by phenotypic noise. *Nature* 454: 987–90.
- Macpherson AJ, Uhr T (2004) Induction of protective IgA by intestinal dendritic cells carrying commensal bacteria. *Science* 303: 1662–5.
- Hapfelmeier S, Müller AJ, Stecher B, Kaiser P, Barthel M, et al. (2008) Microbe sampling by mucosal dendritic cells is a discrete, MyD88-independent step in DeltainvG S. Typhimurium colitis. *J Exp Med* 205: 437–50.
- Müller AJ, Kaiser P, Dittmar KEJ, Weber TC, Haueter S, et al. (2012) *Salmonella* gut invasion involves TTSS-2-dependent epithelial traversal, basolateral exit, and uptake by epithelium-sampling lamina propria phagocytes. *Cell Host Microbe* 11: 19–32.

Figure S3 State probabilities p_k as functions of time. For this figure we assumed $r=3/d$, $c=0.5/d$, and $\mu_W=1/d$.

(PDF)

Figure S4 Contour plots of likelihood for the different experiments. The red dots indicate the maximum of the likelihood.

(PDF)

Figure S5 Relation between assumed clearance rate constant, c_{fix} , and our parameter estimates. A. The relation to the estimate of the replication rate constant, r . The dashed line shows the expectation under constant net replication rate $\Delta r=r-c$. **B.** The relation to the estimate of the migration rate constant of WITS, μ_W .

(PDF)

Acknowledgments

We would like to thank Tanja Stadler for guidance on how to derive the probability generating function for our stochastic model (Equation 3), and Roger Kouyos for calculating the state probabilities in closed form (Equation 4).

Author Contributions

Conceived and designed the experiments: PK ES WDH RRR. Performed the experiments: PK ES. Analyzed the data: PK ES WDH RRR. Contributed reagents/materials/analysis tools: AJG. Wrote the paper: PK ES AJG WDH RRR.

28. Förster R, Schubel A, Breitfeld D, Kremmer E, Renner-Müller I, et al. (1999) CCR7 coordinates the primary immune response by establishing functional microenvironments in secondary lymphoid organs. *Cell* 99: 23–33.
29. Niess JH, Brand S, Gu X, Landsman L, Jung S, et al. (2005) CX3CR1-mediated dendritic cell access to the intestinal lumen and bacterial clearance. *Science* 307: 254–8.
30. Diehl GE, Longman RS, Zhang JX, Breart B, Galan C, et al. (2013) Microbiota restricts trafficking of bacteria to mesenteric lymph nodes by CX(3)CR1(hi) cells. *Nature* 494: 116–20.
31. Helaine S, Thompson JA, Watson KG, Liu M, Boyle C, et al. (2010) Dynamics of intracellular bacterial replication at the single cell level. *Proc Natl Acad Sci USA* 107: 3746–51.
32. Brown SP, Cornell SJ, Sheppard M, Grant AJ, Maskell DJ, et al. (2006) Intracellular demography and the dynamics of *Salmonella enterica* infections. *PLoS Biol* 4: e349.
33. Gog JR, Murcia A, Osterman N, Restif O, McKinley TJ, et al. (2012) Dynamics of *Salmonella* infection of macrophages at the single cell level. *J R Soc Interface* 9: 2696–707.
34. Druett HA (1952) Bacterial invasion. *Nature* 170: 288.
35. Halvorson HO (1935) The effect of chance on the mortality of experimentally infected animals. *J Bact* 30: 330–331.
36. Levin BR, Bull JJ (1994) Short-sighted evolution and the virulence of pathogenic microorganisms. *Trends Microbiol* 2: 76–81.
37. Hoiseh SK, Stocker BA (1981) Aromatic-dependent *Salmonella typhimurium* are non-virulent and effective as live vaccines. *Nature* 291: 238–9.
38. Hapfelmeier S, Ehrbar K, Stecher B, Barthel M, Kremer M, et al. (2004) Role of the *Salmonella* pathogenicity island 1 effector proteins SipA, SopB, SopE, and SopE2 in *Salmonella enterica* subspecies 1 serovar Typhimurium colitis in streptomycin-pretreated mice. *Infect Immun* 72: 795–809.
39. Suar M, Periaswamy B, Songhet P, Misselwitz B, Müller A, et al. (2009) Accelerated type III secretion system 2-dependent enteropathogenesis by a *Salmonella enterica* serovar enteritidis PT4/6 strain. *Infect Immun* 77: 3569–77.
40. Pollock JD, Williams DA, Gifford MA, Li LL, Du X, et al. (1995) Mouse model of X-linked chronic granulomatous disease, an inherited defect in phagocyte superoxide production. *Nat Genet* 9: 202–9.
41. Karlin S, Taylor HM (1975) *A first course in stochastic processes*, Academic Press, chapter 4. Second edition.
42. Debnath L (2012) *Nonlinear Partial Differential Equations for Scientists and Engineers*. Birkhäuser Boston, third edition.
43. Read T, Cressie N (1988) *Goodness-of-Fit Statistics for Discrete Multivariate Data*. Springer Series in Statistics. Springer.
44. R Development Core Team (2010) *R: A Language and Environment for Statistical Computing*. R Foundation for Statistical Computing, Vienna, Austria. URL <http://www.R-project.org>. ISBN 3-900051-07-0.
45. Pineda-Krch M (2010) GillespieSSA: a stochastic simulation package for R .